

Boundary-induced effect encoded in the corrections to the geometric phase acquired by a bipartite two-level system

Ludmila Viotti, Fernando C. Lombardo and Paula I. Villar¹

¹*Departamento de Física Juan José Giambiagi, FCEyN UBA and IFIBA CONICET-UBA, Facultad de Ciencias Exactas y Naturales, Ciudad Universitaria, Pabellón I, 1428 Buenos Aires, Argentina.*

(Dated: September 12, 2022)

We present a bipartite two-level system coupled to electromagnetic quantum vacuum fluctuations through a general dipolar coupling. We derive the master equation in the framework of open quantum systems, assuming an environment composed of (i) solely vacuum fluctuations and (ii) the vacuum fluctuations and a conducting plate located at a fixed distance from the bipartite system. For both cases considered, we study the dynamics of the bipartite system and the temporal evolution of the concurrence of an initial entangled bipartite state. We further analyze the generation of entanglement due to the vacuum structure. Finally, we study the different induced contributions to the correction of the unitary geometric phase of a bipartite quantum state so as to explore the possibility of future experimental setups by considering the influence of boundaries conditions in vacuum.

PACS numbers:

I. INTRODUCTION

The global phase acquired by a quantum system due to its dynamical evolution contains a gauge-invariant component, namely, the geometric phase (GP) which depends only on the geometry of the path traversed by the system during the quantum evolution [1, 2]. Due to the fact that a quantum system unavoidably interacts with its environment and undergoes decoherence, much attention has been raised by studies on the geometric phase in open quantum systems under non-unitary dynamics [3–9]. Moreover, the geometric phase acquired in a quantum evolution has been observed and measured in a variety of experiments [10, 11], and it has been demonstrated that its geometric nature has potential applications in inferring quantum properties of the systems. It has also been suggested as a measure of the Unruh effect at lower accelerations [12–14]. Recently, it has even been proposed to track traces of quantum friction in the case of an atom coupled to a scalar quantum field, traveling at constant velocity at a fixed distance in front of a dielectric plate [15]. Another major concept in quantum physics happens to be that of entanglement, playing a central role in many novel quantum technologies [16, 17]. It has been said that two initially entangled atoms may get completely disentangled within a finite time, which is known as entanglement sudden death [18]. Likewise, a common bath can also provide indirect interactions among independent atoms, leading to entanglement sudden birth [19, 20]. Thus, the definition and modeling of the environment becomes of prime relevance in the study of quantum entanglement [21, 22]. In particular, vacuum quantum fluctuations are a type of environment that can not be turned off. It is well known that electromagnetic quantum fluctuations are modified by the presence of boundaries and the resulting distortions are known as observable effects such as the Lamb shift [23] and the Casimir effect [24].

The GP has been studied for bipartite systems in

[25, 26], showing that an initially maximally entangled (MES) state acquired a “robust” GP. As the GP is known to be less corrected in a MES state for the spin-boson model [25], we shall extend the study of the corrections to the GP to a bipartite state coupled to electromagnetic vacuum fluctuations. In this context, questions also naturally arise as to what happens to the geometric phase acquired by a quantum system by the presence of boundary effects. Furthermore, it may be useful to know if the influence of these boundaries can be exploited for an experimental test on the GP as so to infer quantum properties of the systems.

This paper is structured as follows. In Section II, we present the model studied and derive the master quantum equation so as to describe the dynamics of two two-level systems coupled to electromagnetic quantum vacuum fluctuations through a dipolar coupling. We derive the environmental kernels for two situations: (i) free space vacuum fluctuations and (ii) a conducting plate located at a fixed distance of the bipartite quantum system. In Sec. III we study the dynamics of an initially entangled state under the presence of quantum vacuum fluctuations, focusing on the effect when boundaries are considered. In Sec. IV, we extend the analysis to the entanglement dynamics of the bipartite system, by considering how the initial entanglement of the quantum system is influenced by the environment. Further, we study if the presence of the environment can generate entanglement in an initial separable state and the functional dependence of the concurrence upon the distance to the conducting plate and the distance among particles. In Sec. V we compute the GP acquired by the bipartite system in either situation considered, in order to compare both situations and see if the presence of boundaries conditions can be exploited for future measurements the GP. Finally, in Sec. VI, we summarize the results and present conclusions.

II. THE SYSTEM

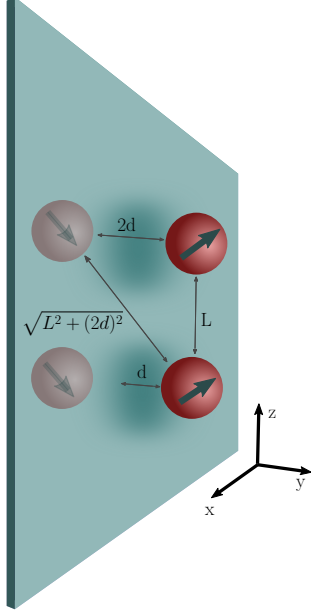


FIG. 1: A scheme of the system under consideration, where the two-level atoms are at a fixed distance d from a perfectly conducting plate and separated by a distance L . The electromagnetic field in presence of a conducting plate, can be thought of as that produced by the atoms and two image dipoles.

We shall consider a bipartite system consisting in two, originally non-interacting, two-level systems. Both two level systems are coupled to the electromagnetic field in its vacuum state (and all in turn can be in presence of a perfectly conducting plate). The model, which is schematically represented in Fig. 1, can be mathematically described by a Hamiltonian

$$H = H_s + H_{\text{em}} + H_{\text{int}}, \quad (1)$$

where the first two terms H_s and H_{em} are the Hamiltonian of the free bipartite system and the electromagnetic field in presence of a perfectly conducting plate respectively, and H_{int} is the interaction Hamiltonian between the system and the vacuum field. The free system Hamiltonian can be written as

$$H_s = \frac{\hbar}{2}\omega_0^1\sigma_3^1 + \frac{\hbar}{2}\omega_0^2\sigma_3^2, \quad (2)$$

while the interaction Hamiltonian can be expressed as $H_{\text{int}} = H_{\text{int}}^1 + H_{\text{int}}^2$, with

$$\begin{aligned} H_{\text{int}}^i &= -e \hat{\mathbf{r}}^i \cdot \hat{\mathbf{E}}(t, x^i) \\ &= -e \sum_{\lambda=1}^2 \int \frac{d^3k}{(2\pi)^3} \sqrt{2\pi\hbar\omega_{\mathbf{k}}} (\mathbf{r}_+^i \sigma_+^i + \mathbf{r}_-^i \sigma_-^i) \\ &\quad \times [a_{\lambda\mathbf{k}} A_{\lambda\mathbf{k}}(\mathbf{x}^i) - a_{\lambda\mathbf{k}}^\dagger A_{\lambda\mathbf{k}}^*(\mathbf{x}^i)] \epsilon_{\lambda\mathbf{k}}. \end{aligned} \quad (3)$$

We have therefore used the lower order multipolar Hamiltonian, with e the electron charge, $e\mathbf{r}$ the atomic electric dipole and the mode functions $A_{\lambda\mathbf{k}}(\mathbf{x})$ of the electromagnetic field, which should be chosen as to satisfy the boundary conditions [27]. The free space mode functions should satisfy the boundary condition,

$$A_{\lambda\mathbf{k}}(\mathbf{x}^i) = e^{-i\mathbf{k}\mathbf{x}^i}, \quad (4)$$

while the functions considering the plate, in the region $y \geq 0$ are

$$A_{1\mathbf{k}}(\mathbf{x}^i) = \sqrt{2} (\hat{k}_{\parallel} \times \hat{k}_{\perp}) e^{i\mathbf{k}_{\parallel}\mathbf{x}_{\parallel}^i} \quad (5)$$

$$A_{2\mathbf{k}}(\mathbf{x}^i) = \frac{\sqrt{2}}{k} \left[k_{\parallel} \cos(\mathbf{k}_{\perp}\mathbf{x}_{\perp}^i) \hat{k}_{\perp} - i k_{\perp} \sin(\mathbf{k}_{\perp}\mathbf{x}_{\perp}^i) \hat{k}_{\parallel} \right],$$

with $\mathbf{x}^1 = (0, d, L)$, $\mathbf{x}^2 = (0, d, 0)$, $\mathbf{k}_{\parallel} = (k_1, 0, k_3)$ and $\mathbf{k}_{\perp} = k_2 \hat{y}$.

As we want to know the dynamics of the bipartite system at all times, we shall derive a master quantum equation by applying the formalism of open quantum systems [28]. The state of the system, which is represented by the reduced density matrix for the bipartite system, satisfies a master equation. If we perform a power expansion, up to second order in series of the coupling between the bipartite system and the environment (composed by the electromagnetic field plus the mirror), this equation is given by

$$\begin{aligned} \dot{\rho}_s(t) &= \frac{1}{i\hbar} \text{Tr}_{\epsilon} ([V(t), \rho_s(t) \otimes \rho_{\epsilon}]) \\ &\quad - \frac{1}{\hbar^2} \int_0^t dt' \text{Tr}_{\epsilon} ([V(t), [V(t'), \rho_s(t) \otimes \rho_{\epsilon}]] \\ &\quad + \frac{1}{\hbar^2} \int_0^t dt' \text{Tr}_{\epsilon} ([V(t), \text{Tr}_{\epsilon} ([V(t'), \rho_s(t) \otimes \rho_{\epsilon}]) \otimes \rho_{\epsilon}]) \end{aligned} \quad (6)$$

where $V(t) = U_0^\dagger H_{\text{int}} U_0$ is the interaction Hamiltonian in the interaction picture and $U_0 = e^{-\frac{i}{\hbar}(H_s + H_{\epsilon})t}$ is the operator representing the evolution produced by the free theories. By taking the initial state of the electromagnetic field to be the vacuum state, both the first and the third terms in Eq. (6) vanish, leaving a simplified equation governing the dynamics of the bipartite system:

$$\dot{\rho}_s(t) = -\frac{1}{\hbar^2} \int_0^t dt' \text{Tr}_{\epsilon} ([V(t), [V(t'), \rho_s(t) \otimes \rho_{\epsilon}]]). \quad (7)$$

The interaction $V(t)$ present in Eq. (7) can be found through a simple calculation involving Hausdorff formula, resulting in

$$\begin{aligned} V^i(t) &= -e \sum_{\lambda=1}^2 \int \frac{d^3k}{(2\pi)^3} \sqrt{2\pi\hbar\omega_{\mathbf{k}}} \\ &\quad \times \left[\mathbf{r}_+^i (\sigma_+^i \otimes a_{\lambda\mathbf{k}}) A_{\lambda\mathbf{k}}(\mathbf{x}^i) e^{-i(\omega_{\mathbf{k}} - \omega_0^i)t} + \right. \\ &\quad \mathbf{r}_+^i (\sigma_+^i \otimes a_{\lambda\mathbf{k}}^\dagger) A_{\lambda\mathbf{k}}^*(\mathbf{x}^i) e^{i(\omega_{\mathbf{k}} + \omega_0^i)t} + \\ &\quad \mathbf{r}_-^i (\sigma_-^i \otimes a_{\lambda\mathbf{k}}) A_{\lambda\mathbf{k}}(\mathbf{x}^i) e^{-i(\omega_{\mathbf{k}} + \omega_0^i)t} + \\ &\quad \left. \mathbf{r}_-^i (\sigma_-^i \otimes a_{\lambda\mathbf{k}}^\dagger) A_{\lambda\mathbf{k}}^*(\mathbf{x}^i) e^{i(\omega_{\mathbf{k}} - \omega_0^i)t} \right] \epsilon_{\lambda\mathbf{k}}. \end{aligned} \quad (8)$$

With Eqs. (7) and (8) as the starting point and after some algebra, the master equation governing the dynamics of the reduced density matrix for the bipartite system can be written, in the secular approximation:

$$\begin{aligned} \dot{\rho}_s(t) = & \frac{1}{i\hbar} [H_s, \rho_s] \\ & - \sum_{i,j=1}^2 \left[\int_0^t dt_1 K_-^{ij}(t') \left([\sigma_+^i, \{\sigma_-^j, \rho_s\}] + [\sigma_+^i, [\sigma_-^j, \rho_s]] \right) + \right. \\ & \left. \int_0^t dt_1 K_+^{ij}(t') \left([\sigma_-^i, \{\sigma_+^j, \rho_s\}] + [\sigma_-^i, [\sigma_+^j, \rho_s]] \right) + \text{h.c.} \right], \end{aligned} \quad (9)$$

valid as long as the relaxation time τ_R and all evolution timescales of the system $\tau_S \sim 1/\omega_0^i$ satisfy the relation $\tau_R \gg \tau_S$ [28]. $K_{\pm}^{ij}(t')$ are kernels containing all the information about the effect of the electromagnetic field on the system.

$$\begin{aligned} K_{\pm}^{ij}(t') = & 2\pi \frac{e^2}{\hbar} |\mathbf{r}|^2 \sum_{m,n=1}^3 r_m^i r_n^j \int \frac{d^3\mathbf{k}}{(2\pi)^3} \omega_{\mathbf{k}} \\ & \times \left(\sum_{\lambda} A_{\lambda\mathbf{k}}(\mathbf{x}^i) A_{\lambda\mathbf{k}}^*(\mathbf{x}^j) \right) e^{-i(\omega_{\mathbf{k}} \pm \omega_0)(t-t')}. \end{aligned} \quad (10)$$

In order to obtain these kernels we have made some further assumptions. We are assuming that both atoms have the same natural frequency ω_0 and that they have the same dipolar moment magnitude $|\mathbf{r}|$ allowing for the moment the directions to be different. These directions are represented by two unit vectors \hat{r}^i whose components are r_m^i . The master equation can be written in a more suggestive form

$$\begin{aligned} \dot{\rho}_s(t) = & \frac{1}{i\hbar} [H_s, \rho_s] - i \sum_{i=1}^2 c_{ii}(t) [\sigma_+^i \sigma_-^i, \rho_s] \\ & - i \sum_{i \neq j} c_{ij}(t) \left(\sigma_+^i \sigma_-^j \rho_s - \rho_s \sigma_+^j \sigma_-^i - \sigma_-^j \rho_s \sigma_+^i + \sigma_-^i \rho_s \sigma_+^j \right) \\ & - \sum_{i=1}^2 a_{ii}(t) \left(\sigma_+^i \sigma_-^i \rho_s + \rho_s \sigma_+^i \sigma_-^i - 2\sigma_-^i \rho_s \sigma_+^i \right) \\ & - \sum_{i \neq j} a_{ij}(t) \left(\sigma_+^i \sigma_-^j \rho_s + \rho_s \sigma_+^j \sigma_-^i - \sigma_-^j \rho_s \sigma_+^i - \sigma_-^i \rho_s \sigma_+^j \right). \end{aligned} \quad (11)$$

The first term corresponds to the free evolution of the system (unitary evolution) while the second and third terms are the frequency renormalization and an effective interaction terms, respectively. The last two terms in this equation are responsible for dissipation and fluctuations (noise) effects. In the previous equation we have used that $\sigma_{\pm} = \sigma_x \pm i\sigma_y$. The information about the environment (with or without boundaries) is thus encoded in the kernels $a_{ij}(t)$ and $c_{ij}(t)$, which in the markovian approximation can be computed by direct integration as

$$a_{ij} = \text{Re} \int_0^\infty dt' K^{ij}(t'), \quad (12)$$

$$c_{ij} = i \neq j \text{Im} \int_0^\infty dt' \left(K_+^{ij}(t') + K_-^{ij}(t') \right), \quad (13)$$

$$c_{ii} = \text{Im} \int_0^\infty dt' \left(K_+^{ii}(t') - K_-^{ii}(t') \right), \quad (14)$$

It is easy to note in Eq.(11) that the coefficient c_{ii} represents a frequency renormalization, while the term with $c_{ij}, i \neq j$ is an effective dipole interaction between the atoms. The coefficient $a_{ij}, i \neq j$ is usually referred to as collective damping. It is important to note, that the kernels will have different expressions whether we are considering the bipartite system either in free space (solely coupled to quantum vacuum fluctuations) or the presence of a perfectly reflecting boundary in quantum vacuum. The explicit expression for the environment $a_{ij}(t)$ and $c_{ij}(t)$ kernels can be found in Appendix A, and will remain valid as long as markovian approximation does. This is, as long as the relaxation time τ_R and the vacuum field correlation time τ_E (the characteristic width of the environment correlation functions) satisfy the condition $\tau_R \gg \tau_E$, which imposes the conditions, in natural units, $L\omega_0 \gtrsim 1$ and $2d\omega_0 \gtrsim 1$ [29].

Finally, by assuming that $K^{12}(t) = K^{21}(t)$ and $K^{11}(t) = K^{22}(t)$, the master equation derived can be analytically solved for a general initial state of the bipartite qubit system of the form

$$|\psi\rangle = \alpha |11\rangle + \beta |10\rangle + \gamma |01\rangle + \sigma |00\rangle. \quad (15)$$

The resulting matrix elements composing the reduced density matrix $\rho_s(t)$ are explicitly given in Appendix B.

III. SYSTEM'S OPEN DYNAMICS: IN FREE SPACE AND WITH A REFLECTING BOUNDARY

We shall start studying the dynamical properties of the system, whether the bipartite system is in free space or at a fixed distance of a reflecting plate, located at $y = 0$. In both cases, the atoms are separated a distance L in \hat{z} direction. If we consider the presence of a plate, we shall also assume the atoms to be fixed at a distance d from the perfectly conducting plate in the \hat{y} direction. As we are interesting in the effect of the vacuum fluctuations (either dressed or undressed) on an initial state of the quantum system, we shall define an initial bipartite state of the form

$$|\psi(0)\rangle = \sqrt{p} |11\rangle + \sqrt{1-p} |00\rangle, \quad (16)$$

in the $\{|00\rangle, |01\rangle, |10\rangle, |11\rangle\}$ basis. In Eq.(16), p determines the degree of entanglement being $|0\rangle$ and $|1\rangle$ eigenstates of the Pauli operator σ_z (of each two level system).

It is easy to note that $p = 1/2$ accounts for a maximally entangled state (MES). As has been indicated in [19], there is no entanglement sudden death for any generic state with maximum one excitation. Analogously, entanglement can be smoothly generated but it cannot suddenly appear. That is the reason we shall limit to study this type of Bell-like state. Taking this particular initial state, the reduced density matrix of the bipartite system assumes the simplified form

$$\rho(t) = \begin{pmatrix} \rho_{11}(t) & 0 & 0 & \rho_{14}(t) \\ 0 & \rho_{22}(t) & \rho_{23}(t) & 0 \\ 0 & \rho_{32}(t) & \rho_{33}(t) & 0 \\ \rho_{41}(t) & 0 & 0 & \rho_{44}(t) \end{pmatrix}.$$

Full expressions of the components of the reduced density matrix can be found in Appendix B. As decoherence is the dynamical suppression of quantum coherences, the off-diagonal elements of the reduced density matrix are a good measure of how the environment affects the dynamics of the system. In our study, the only off-diagonal elements of interest are $\rho_{23}(t)$ and $\rho_{41}(t)$, being the remaining off-diagonal elements either zero, or determined by these two. In what follows, we will be working in natural units $c = \hbar = 1$ and, in this units, we will take the dipolar coupling to be of the order of Bohr radius $|\mathbf{r}| \sim a_0$ and the natural frequency to be of the order of the hydrogen ground state energy $\omega_0 \sim E_0 = 10^6 / 1/m$ leading to $\gamma_0 = 1$ and allowing for expansions in powers of γ_0/ω_0 and satisfying all the approximations that have been done.

In Figs. 2 and 3, we show the evolution of the absolute value of the coherences with time. In each figure, we compare the temporal evolution of the coherences of the reduced density matrix when there is no plate present (solid line). In addition, we show the behavior of these quantities if there is a conducting boundary located at different distances (dotted and dashed lines) from the bipartite quantum system. In the latter case, we can further consider the orientation of the dipolar moment of the atoms. Hence, in both figures, we plot the temporal behavior for perpendicular orientation of both dipole moments on top, and parallel orientation of both atoms at the bottom. As expected, both coherences decay for sufficiently long times in all considered cases. Even yet, the effect introduced by the presence of the plate tends to vanish as the atoms are placed at larger distances, leaving decoherence effects solely to the zero point fluctuations of the electromagnetic field. However, we can note different decoherence timescales for the cases considered. We can surely define the decoherence timescale where interference terms vanish. As it can be seen in Fig.2, vacuum fluctuations induced interference destruction around $\tau \sim 10^6$. If we consider this decoherence time τ_0 as a reference timescale, we can note that decoherence occurs for shorter times when the dipole orientations are perpendicular to the plate (τ_\perp). On the other hand, if orientations are parallel to the boundary, decoherence of the off-diagonal matrix elements takes longer τ_\parallel . Therefore,

we can state that $\tau_\perp < \tau_0 < \tau_\parallel$. In addition, we can further interpret this result in terms of the images method when the bipartite atom system is very close to the conducting surface. If the plane is parallel to the dipole, the image dipole is given by $\mathbf{p}_{\text{im}} = -\mathbf{p}$. Therefore, the total dipole moment vanishes, and so does the probability to emit a photon. The image dipole cancels the effect of the real dipole and this produces less decoherence. On the other hand, when the conductor is perpendicular to the dipolar orientation, the image dipole is equal to the real dipole. Therefore, the total dipole is twice the original one. This in principle would lead us to conclude that the total decoherence factor grows [30].

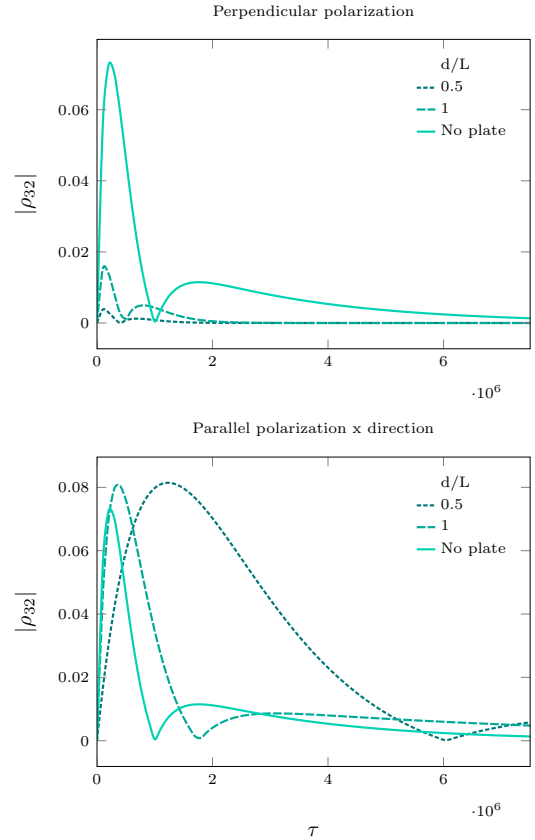


FIG. 2: ρ_{32} absolute value evolution. The solid line represents the behavior when the bipartite system is solely coupled to vacuum fluctuations. Other lines account for the bipartite coupled to vacuum fluctuations at a fixed distance d of a conducting plate: dotted line for $d/L = 0.5$ while dashed line for $d/L = 1$. The bipartite initial state is a maximal entangled state ($p = 1/2$). On top we consider both atoms with perpendicular dipole moment while at bottom, we represent the temporal evolution if both atoms have dipolar moments parallel to the plate.

We can acquire a better picture of the behavior of decoherence with the atom-plate distance by comparing the decoherence process in free space (without plate) with that case in which the vacuum field state is modified by the presence of the boundary condition imposed by the

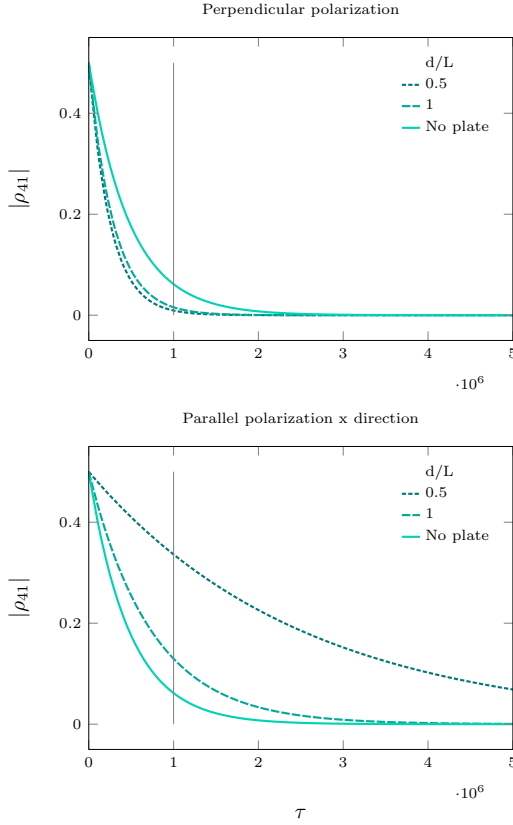


FIG. 3: Evolution of ρ_{41} absolute value. The solid line represents the behavior when the bipartite system is solely coupled to vacuum fluctuations. Other lines account for the bipartite coupled to vacuum fluctuations at a fixed d distance of a conducting plate: dotted line for $d/L = 0.5$ while dashed line for $d/L = 1$. The bipartite initial state is a maximal entangled state ($p = 1/2$). On top we consider both atoms with perpendicular dipole moment while at bottom, we represent the temporal evolution if both atoms have dipolar moments parallel to the plate.

mirror. The results of this comparison, that has been separately done for the elements ρ_{32} and ρ_{41} . As it is suggested from the behavior of $|\rho_{41}|$ seen in Fig. 3, by taking the difference in this element's amplitude at a fixed time when the system is affected by free space electromagnetic field and by the electromagnetic field in presence of a perfectly conducting plate, we could acquire an idea of the relation between the effect of the environment in both cases. This difference

$$\Delta|\rho_{41}| = \left(|\rho_{41}^{\text{plate}}| - |\rho_{41}^{\text{free}}| \right)_{(t=\pi)} \quad (17)$$

is illustrated in the upper figure of Fig. 4 for both x and y polarized atoms. As it will be a recurrent behavior along this work, there is an initial regime in which the presence of the plate reinforces the effect of the environment if the atoms are polarized along the perpendicular y-direction and modifies this effect delaying the system behaviour when they are polarized along the parallel x-

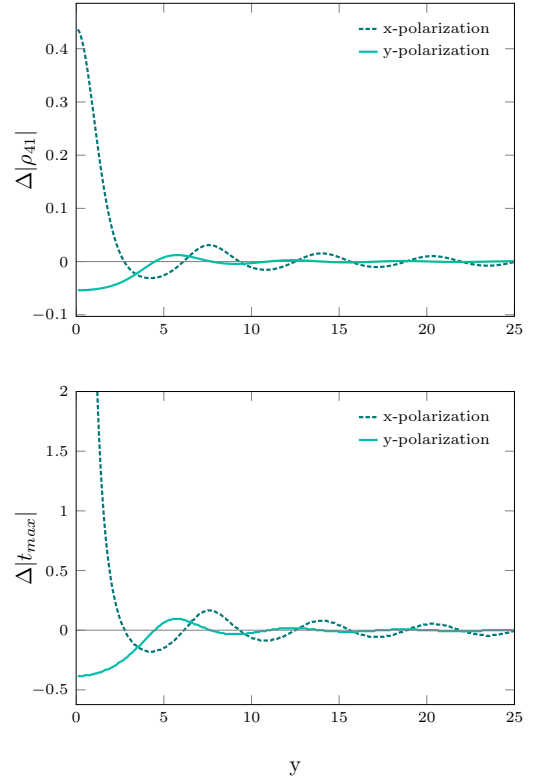


FIG. 4: Comparison between the amplitude decay of the off-diagonal terms of the density matrix as a function of the adimensional distance $y = 2d\omega_0$ between the bipartite system and the plate.

direction. This can be seen as, for a fixed time $t = \pi$ if the amplitude of the element has decreased more in presence of the plate than it would have in the free space case, then Eq. (17) should be negative, obtaining positive values of this subtraction in the opposite case (this fact can be seen for distances d satisfying $d \leq 4L$ approximately). The amplitude of this correction can be seen to decay with distance while oscillating and tends asymptotically to the free space case for distances $d \geq 10L$ approximately. Considering the behavior shown by $|\rho_{32}|$ in Fig. 2, a subtraction similar to that performed for $|\rho_{41}|$ doesn't seem to be a good indicator of the modifications to the environment effect which are introduced by the presence of the plate. Instead, we have plotted the difference in time position of the local maximum present in the revival

$$\Delta t_{\text{max}} = t_{\text{max}}^{\text{plate}} - t_{\text{max}}^{\text{free}}. \quad (18)$$

The lower graph in Fig. 4 consists on a plot of this difference Δt_{max} as a function of the distance from the particles to the plate. We can see that in this case the modification induced by the plate exhibits the same qualitative behavior as that found for $|\rho_{41}|$.

IV. ENTANGLEMENT DYNAMICS

Entanglement is one of the most intriguing properties of quantum mechanics, as it is a form of correlation that can not be explained in terms of any classical theory. Bipartite entanglement of pure states is conceptually well understood. When dealing with mixed states, we say that the state is entangled if it can not be written as a mixture of separable pure states. Among the many physically motivated measures of entanglement for mixed states, entanglement of formation is intended to quantify the resources needed to create a given entangled state, but its exact computation involves a minimization over all possible pure-states decompositions which makes it inconvenient in the general case. However, in the particular case of a bipartite system consisting on two two-level subsystems, the quantity known as concurrence is monotonically related to entanglement of formation and, while its not so clearly motivated, can be taken as a measure of entanglement on its own [31]. The concurrence for the state described by $\rho_s(t)$ vanishes if $\rho_s(t)$ is a separable state and ranges monotonically to 1 for maximally entangled states. It can be computed as

$$\mathcal{C}(\rho) = \max(0, \sqrt{\lambda_1} - \sqrt{\lambda_2} - \sqrt{\lambda_3} - \sqrt{\lambda_4}), \quad (19)$$

where λ_i are the eigenvalues of $\tilde{\rho} = \rho_s^*(\sigma^1 \otimes \sigma^2) \rho_s (\sigma^1 \otimes \sigma^2)$.

In Fig.5, we show the temporal evolution of concurrence for a bipartite initial state of the form defined in Eq.(16). On top of the figure, we can see the concurrence for a maximal entangled state for different situations considered: solely vacuum fluctuations (solid line), parallel dipole orientation (dashed line), perpendicular dipole orientation (dotted line) and an isotropic orientation (dotdashed line). Therein, we can note that concurrence tends to zero following the decoherence timescales hierarchy found before: entanglement of an initially entangled state is faster destroyed when the two atoms' dipole moments are perpendicular oriented to the plane compared to the presence of solely vacuum fluctuations and dipole moments orientations parallel to the plane. For some dipole orientations a revival of entanglement is seen, although its magnitude is much smaller than the initial value. At the bottom of Fig.5, we present the temporal evolution of the concurrence induced by the environment in an initially separate bipartite state for the same situations considered on top. Therein, we can see that the strongest environment (dotted line) is not efficient enough to induce quantum entanglement (at least in the timescale shown). However, if a much weaker environment is considered, we can find that there is sudden generation of entanglement. It is easy to note, that the timescale at which entangled is created follows the inverse of the decoherence timescales hierarchy mentioned before. The existence of entanglement revivals and the entanglement generation should not be thought of as a sign of non-markovianity, as we have discarded all contributions from environmental memory effects when performing the markovian approximation. These features of

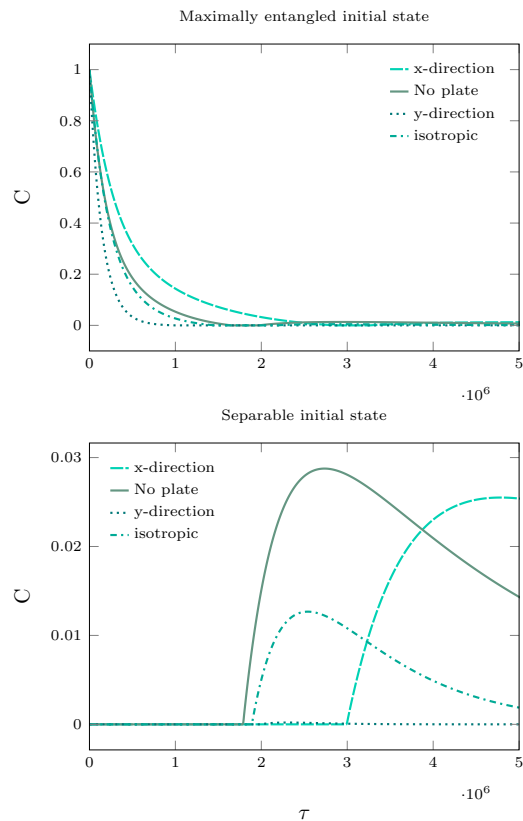


FIG. 5: Temporal evolution of concurrence when the system is coupled to vacuum fluctuations (solid line) and coupled to vacuum fluctuations at a fixed distance of a plate. Dipole perpendicular orientation is represented with a dotted line while parallel dipole orientation is represented with a dashed line. Top: Initial maximal entangled state ($p=0.5$). Bottom: Initial separable state ($p=1$).

entanglement dynamics are a consequence of the induced collective dynamics [20, 32]. The radiated field produced by spontaneous emission of an atom influences the dynamics of the other atom through the vacuum field, but there is no information backflow from the field to the radiating atom.

In Fig.6, we present the temporal evolution of the concurrence for a maximally entangled state ($p = 0.5$) as function of the distance to the conducting plate d for two different situations: (top) perpendicular-aligned atoms and (bottom) parallel-aligned atoms. In Fig.7, we plot the induced entanglement generation for an initially separate state for different distances of the bipartite to the plate. Therein, it is easy to note that entanglement birth is more likely to occur when the dipoles are oriented parallel to the conducting plate. On top of Fig.7, we can see that for short distances to the plate, no entanglement generation is induced when the dipoles are oriented perpendicular to the plate. It can be seen that this correction tends to delay the revival for atoms polarized along the x-direction, while it is suppressed for atoms polarized along the perpendicular y-direction. By exploring

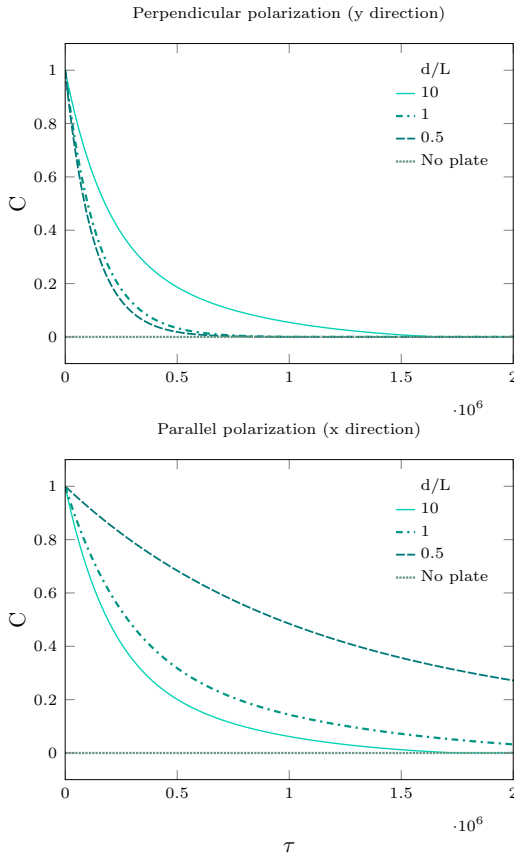


FIG. 6: Concurrence evolution for an initial maximally entangled state ($p=0.5$), considering the atoms fixed at different distances of the conducting plate. Top: perpendicular dipole orientation. Bottom: parallel dipole orientation.

the dependence of this correction with the distance from the atoms to the plate, as it is shown in Fig. 6, we found that the revival is suppressed for atoms polarized along the perpendicular direction when they are placed close to the plate, appearing as the distance is increased. When the dipolar coupling is along the x-direction, the presence of the plate seems to delay the appearance of the revival and extend its duration. Even when this behavior is not monotonic with distance, it can be seen that it is indeed monotonic for those distance intervals for which the correction is stronger.

V. GEOMETRIC PHASE

In this section we shall study the geometric phase accumulated by the bipartite system when evolving under the presence of vacuum fluctuations. We shall study the corrections to the unitary geometric phase acquired and compared it with that obtained when there is a conducting plate. The geometric phase for a mixed state under non-unitary evolution has been defined in the kinematic approach as [33, 34]

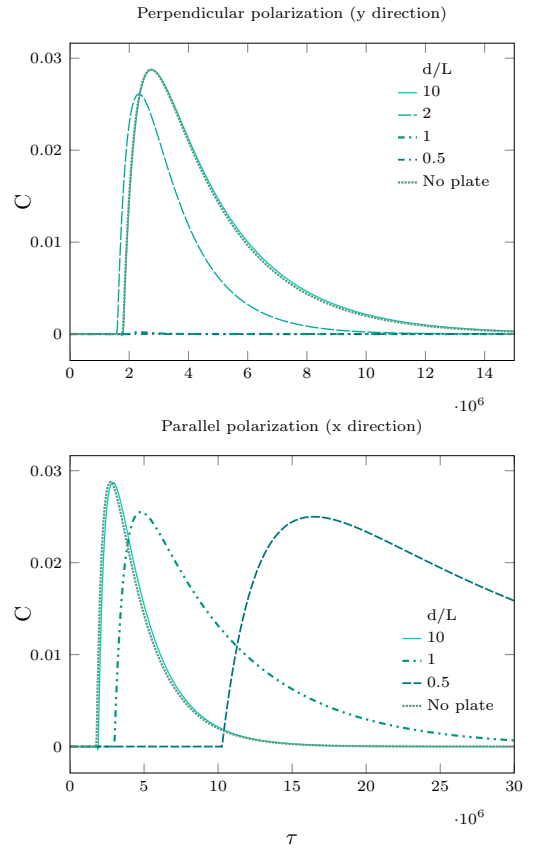


FIG. 7: Concurrence evolution (as a function of natural periods) for an initial separable state ($p=1$), considering the atoms fixed at different distances of the conducting plate. Top: perpendicular dipole orientation. Bottom: parallel dipole orientation.

$$\phi_g = \arg \sum_k \sqrt{\epsilon_k(0)\epsilon_k(\tau)} \langle \Psi_k(0) | \Psi_k(\tau) \rangle e^{-\int_0^\tau dt \langle \Psi_k | \dot{\Psi}_k \rangle},$$

where $\epsilon_k(t)$ are the eigenvalues and $|\Psi(t)\rangle$ are the eigenstates of $\rho_s(t)$. For a pure initial state, the expression above is simplified to

$$\phi_g = \arg \langle \Psi(0) | \Psi(\tau) \rangle - \text{Im} \int_0^\tau dt \langle \Psi | \dot{\Psi} \rangle, \quad (20)$$

with $|\Psi(t)\rangle$ the eigenstate associated to the eigenvalue $\lambda(t)$ that satisfies $\lambda(0) = 1$. In the last definition, τ denotes a time after the total system completes a cyclic evolution when it is isolated from the environment. Taking into account the effect of the environment, the system no longer undergoes a cyclic evolution. However, we shall consider a quasi cyclic path for a time interval $t \in [0, \tau]$ with $\tau = \pi/\omega_0$. When the system is open, the geometric phase that would have been obtained if the system had been closed ϕ_u is modified. This means, in a general case, the phase is $\phi_g = \phi_u + \delta\phi$, where $\delta\phi$ is the

correction to the unitary phase, induced by the presence of the environment (electromagnetic field and conducting plate) [3]. The eigenvalues of the reduced density matrix of the system can be found to be

$$\lambda_{\pm}^1 = \frac{1}{2} \left(\rho_{11} + \rho_{44} \pm \sqrt{(\rho_{11} - \rho_{44})^2 + 4|\rho_{41}|^2} \right)$$

$$\lambda_{\pm}^2 = \frac{1}{2} \left(\rho_{22} + \rho_{33} \pm \sqrt{(\rho_{22} - \rho_{33})^2 + 4|\rho_{32}|^2} \right),$$

and it is easy to see that $\lambda_+^1(0) = 1$ while the rest of the eigenvalues vanish at $t = 0$. The eigenstate appearing in Eq.(20) is then

$$|\Psi\rangle = \frac{-(\rho_{44} - \lambda_+^1)|11\rangle + \rho_{41}|00\rangle}{\sqrt{(\rho_{44} - \lambda_+^1)^2 + |\rho_{41}|^2}}. \quad (21)$$

With this eigenstate, Eq.(20) reduces to the integral

$$\phi_g = -(\omega_0 + c_{11}) \int_0^\tau \frac{|\rho_{41}|}{(\rho_{44} - \lambda_+^1)^2 + |\rho_{41}|^2} d\tau. \quad (22)$$

We shall start by studying the geometric phase acquired under the influence of the environment. If the correction to the GP is negligible ($\delta\phi \ll \phi_u$), the GP acquired would be very similar to the unitary one $\phi_g \sim \phi_u$, and thus $1 - \phi_g/\phi_u \approx 0$. If the correction becomes considerable, then this quantity would increase. In Fig. 8, we show the GP acquired by an initial maximally entangled state for different winding numbers $N = t/\tau$. On top, we can find the situation where the dipoles are perpendicular-oriented while at bottom, the dipoles are oriented parallel to the plate. In both cases, we show how the correction to the GP is modified as the bipartite system is located at different distances from the plate d/L and compare each case to the correction obtain when the system is only coupled to vacuum fluctuations (solid line). If we choose a fixed time or cycle, i.e. $N = 5$, we can see that the correction to the GP is smaller for small distances to the conducting plate when the dipoles are oriented parallel to the surface. On the contrary, if the dipoles are perpendicular to the surface, the smallest correction belongs to a fixed distance far enough from the plate (as if there were no plate at all). The correction to the GP tends in most cases to be enlarged when compared to the correction induced in the free (no mirror) space when the particles are polarized in the \hat{y} -direction and to be diminished when they are polarized in the parallel \hat{x} -direction, in accordance with the results obtained for the coherences and the concurrence of the state. As expected, these corrections tend to the free space correction for big enough distances in all cases.

In order to obtain an analytical expression of the correction $\delta\phi$ and get an insight into its functional dependence, we can further perform an expansion of this phase

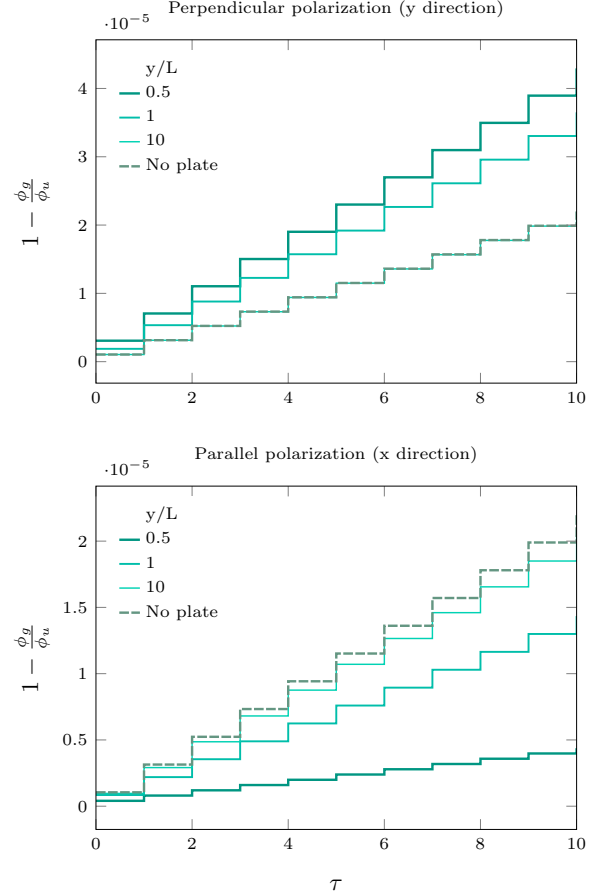


FIG. 8: Correction to the GP as a function of time (measured in natural periods) for different relations of the distance between atoms L and the distance to the plate d , for an initial state with $p=0.5$. Above: atoms polarized perpendicular to the plate. Bottom: atoms polarized parallel to the plate.

for small γ_0/ω_0 (weak coupling limit) up to second order,

$$\phi_g \approx -2\pi(1-p) \left[1 + (c_{11} + 2\pi p a_{11}) \frac{1}{\omega_0} + \right. \quad (23)$$

$$\left. + \frac{2\pi p}{3\omega_0^2} [3a_{11}c_{11} + 4\pi p a_{12}^2 - 4\pi(1-3p)a_{11}^2] \right] + \mathcal{O}\left(\frac{\gamma_0}{\omega_0}\right)^3.$$

The first term in the above expansion is $\phi_u = -2\pi(1-p)$, the unitary geometric phase (this is the phase we would have obtained when the system is isolated). We can see that the first order correction depends only on a_{11} and c_{11} meaning the correction is, to this order, independent of the separation between the atoms L , which contributes only to the following order. However it is not independent of the fact that there are two particles, as it is reflected in the quadratic dependence of the first order correction, compared to the cubic dependence found in works previously done [25, 35]. Further analysis can be done over the phase if we write the expressions for a_{11} and c_{11} so

that the correction, to first order in γ_0/ω_0 reads

$$\delta\phi \approx -4\pi^2(1-p)p\frac{\gamma_0}{\omega_0}\left[1 - 3\sum_{m=1}^3(r_m^1)^2\left(b^{11}(d,\omega_0) - \frac{h^{11}(d,\omega_0)}{2\pi^2p}\right)\right], \quad (24)$$

where it becomes clear that the correction has a free-space component $-4\pi^2(1-p)p$ and a contribution induced by the presence of the plate. The correction to the phase obtained in Eq.(24) has a strong dependence on the distance to the plate at which the atoms are fixed due to the $1/y^3$ dependence of the frequency shift h^{11} . For distances in the considered range the correction takes its maximum value at

$$p = \frac{1}{2} - \frac{3\sum_{m=1}^3(r_m^1)^2 h^{11}(d,\omega_0)}{4\pi^2\left(1 - 3\sum_{m=1}^3(r_m^1)^2 b^{11}(d,\omega_0)\right)}. \quad (25)$$

for any polarization. For this last particular case (25) there is a maximum correction to the phase given by

$$\delta\phi_{\max} = \frac{(2\pi a_{11} + c_{11})^2}{4a_{11}\omega_0}.$$

It is clear that the maximum correction to the phase (to first order in γ_0/ω_0) occurs for the maximally entangled state in the free space case and it is modified by the presence of the conducting plate. In order to get a picture of the range of validity of this approximation we have studied the variation of both the exact phase difference and the first order approximation as a function of the expansion parameter γ_0/ω_0 , as shown in Fig. 9. We did so for different initial states and for both studied polarization directions of the atoms, considering they are fixed at a distance $d = L$ from the plate.

For most studied p -values the first order approximation faithfully reproduces the exact behavior for γ_0/ω_0 values ranging up to 10^{-4} , starting to be distinguishable for γ_0/ω_0 values of order 2.10^{-4} . This range of validity seems to be similar for both polarization directions. The specific case of $p = 0.99$, which represents an initial state very close to $|11\rangle$ exhibits a different behavior as the approximation remains valid for γ_0/ω_0 values up to three times bigger.

VI. CONCLUSIONS

In this article, we have studied the complete dynamics of a bipartite two-level state system (atoms) coupled to an electromagnetic field. We have derived the complete master equation and obtained the reduced density matrix. When computing the environmental kernels for the vacuum fluctuations, we further contemplate the situation of having a conducting plate at a fixed distance d of the bipartite system. In this way, we have obtained environmental kernels comprised of terms depending solely

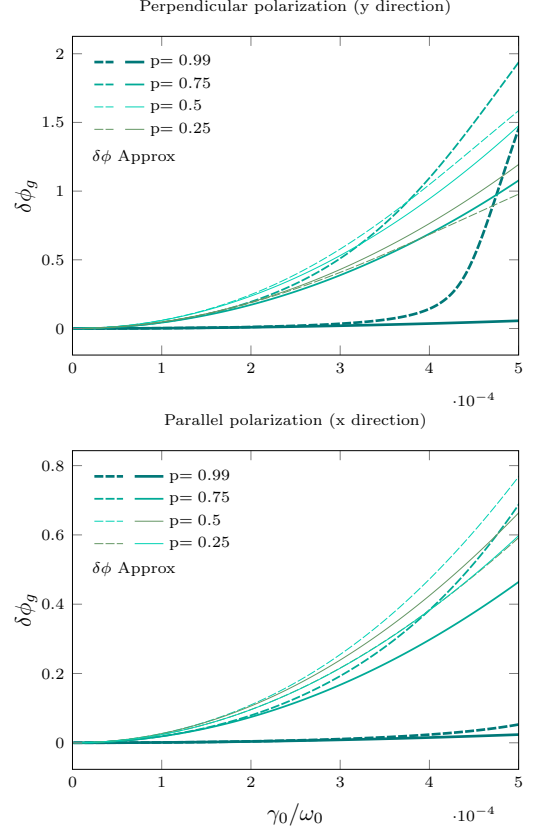


FIG. 9: Exact GP correction as a function of the expansion parameter γ_0/ω_0 compared to first order approximation for different initial states. Top: perpendicular-oriented dipoles. Bottom: parallel-oriented dipoles.

upon vacuum fluctuations and other terms with a clear dependence upon the distance to the plate. Once we have obtained the reduced density matrix for a general state of the bipartite system, we studied the dynamics of a Bell-like initial state. We have defined the decoherence timescale for vacuum fluctuations and compared the decoherence timescale when there is a conducting plate. As for the latter situation, we defined two clearly situations: (i) atomic dipole orientations parallel to the boundary and (ii) atomic dipole orientations perpendicular to the plate. We have obtained that there is a hierarchy in the decoherence timescales for the different situations considered. This result could be easily understood in terms of the image method, concluding that having a dipole orientated perpendicular to the plate, can be demonstrated to originate a more noisy environment and therefore lead to a decoherence timescale shorter than in the case of the dipole is parallel oriented.

Further, we have studied the temporal evolution of concurrence for the initial bipartite state, starting with an entangled initial state. We have also analyzed the creation of entanglement in a separable initial state due to the interaction with the environment. We have found that entanglement is most likely to be created for an ini-

tially separate state if the dipoles are oriented parallel to the surface.

Finally, we have computed the accumulated geometric phase acquired by a bipartite system in the presence of the external environment. We have considered an initial maximally entangled state and studied how the geometric phase is corrected for each case considered, and compared the results to the correction obtained if the bipartite have evolved in free space (only vacuum fluctuations). We have further considered how the GP is corrected if the bipartite state is located at different distances to the plate, finding that it is most corrected for small distances to the plate in the case the dipoles are oriented perpendicular to the boundary. We have also performed an analytical expansion in order to determine the different contributions to the correction of the geometric phase. We have found two types of contribution to the correction of the GP: (i) a contribution induced by vacuum fluctuations and (ii) a contribution induced by the presence of a conducting boundary. This interesting result reinforces the idea that the geometric phase has become a fruitful venue to explore indirectly quantum properties of a system with the emergence of new technologies.

All in all, we have presented a model in which we can exploit the quantum vacuum structure rendering a good scenario for measurements of the geometric phase. It has been argued that the observation of GPs should be done in times long enough to obey the adiabatic approximation but short enough to prevent decoherence from deleting all phase information. This means that while there are dissipative and diffusive effects that induce a correction to the unitary GP, the system maintains its purity for several cycles, which allows the GP to be observed. Particularly, we have shown that if we want to take advantage of the boundary induced structure modification of quantum vacuum, we shall explore an experimental setup at short distance of a reflecting mirror with a bipartite system composed of parallel oriented dipoles. In such a situation, we shall find that the geometric phase acquired is similar to the unitary one at short times.

Acknowledgements

This work was supported by Agencia Nacional de Promocion Cientifica y Tecnologica (ANPCyT), Consejo Nacional de Investigaciones Cientificas y Tecnicas (CONICET), and Universidad de Buenos Aires (UBA), Argentina. FCL acknowledges International Centre for Theoretical Physics and Simons Associate Program.

Appendix A: Environment kernels

The environment $a_{ij}(t)$ and $c_{ij}(t)$ kernels, are defined as:

$$\begin{aligned} a_{ii} &= \gamma_0 \sum_{m=1}^3 (r_m^i)^2 [f^{ii}(\omega_0) - 3b^{ii}(d, \omega_0)] \\ c_{ii} &= -\frac{3\gamma_0}{\pi} \sum_{m=1}^3 (r_m^i)^2 h^{ii}(d, \omega_0) \\ a_{12} &= a_{21} = 3\gamma_0 \sum_{m=1}^3 r_m^1 r_m^2 [f^{12}(L, \omega_0) - b^{12}(L, d)] \\ c_{12} &= c_{21} = 3\gamma_0 \sum_{m=1}^3 r_m^1 r_m^2 [g^{12}(L, \omega_0) - h^{12}(L, d, \omega_0)]. \end{aligned} \quad (A1)$$

In the above set of equations, $\gamma_0 = \frac{|\mathbf{r}|^2 \omega_0^3}{3}$, remembering we're working in natural units $c = \hbar = 1$. Therein, we can identify different contributions of the environment:

- (i) terms derived from solely vacuum fluctuations, such as f^{ii} which does not depend on any distance and represent the effect of the environment as generator of spontaneous emission process.
- (ii) terms derived from solely vacuum fluctuations, such as f^{ij} and g^{ij} , expressed in terms of an adimensional variable $x = L\omega_0$, where L is the distance among quantum particles and represent an effective influence of each particle on the other due to their coupling with the electromagnetic field. This influence manifests itself both in an effective dipole-dipole interaction and in the collective damping factor.
- (iii) terms comprising the presence of the reflecting plate, such as b^{ij} and h^{ij} , expressed in terms of adimensional variables $y = 2d\omega_0$ and $z = \sqrt{x^2 + y^2}$, where d is the distance of both particles to the plate. Those terms depending on $y = 2d$ can be thought as effective actions exerted on an atom by its image dipole while those depending on $z = \sqrt{x^2 + y^2}$, as effective actions exerted on an atom by the image dipole of the other atom. This can be seen from Im.1 where it is clear that those are the distances between the referred particles.

The explicit form of these contributions is:

$$\begin{aligned}
f^{ii} &= 1 \\
b^{ii}(y) &= \frac{\delta_{m1} + \delta_{m3}}{2} \frac{A(y)}{y^3} - \delta_{m2} \frac{B(y)}{y^3} \\
h^{ii}(y) &= \frac{\delta_{m1} + \delta_{m3}}{2y^3} \left[y - \cosint(y) A(y) - \sinint(y) \tilde{A}(y) \right] \\
&\quad - \frac{\delta_{m2}}{y^3} \left[\cosint(y) B(y) - \sinint(y) \tilde{B}(y) \right] \\
f^{12}(x) &= \frac{\delta_{m1} + \delta_{m2}}{2} \frac{A(x)}{x^3} - \delta_{m3} \frac{B(x)}{x^3} \\
b^{12}(z) &= \frac{\delta_{m1}}{2} \frac{A(z)}{z^3} + \delta_{m3} \frac{C(z)}{z^3} - \frac{\delta_{m2}}{2} \frac{D(z)}{z^3} \\
g^{12}(x) &= \frac{\delta_{m1} + \delta_{m2}}{2} \frac{\tilde{A}(x)}{x^3} + \delta_{m3} \frac{\tilde{B}(x)}{x^3} \\
h^{12}(z) &= \frac{\delta_{m1}}{2} \frac{\tilde{A}(z)}{z^3} + \frac{\delta_{m2}}{2} \frac{\tilde{D}(z)}{z^5} + \delta_{m3} \frac{\tilde{C}(z)}{z^5},
\end{aligned}$$

among the definition of the functions appearing therein:

$$\begin{aligned}
A(x) &= x \cos(x) + (x^2 - 1) \sin(x) \\
\tilde{A}(x) &= x \sin(x) - (x^2 - 1) \cos(x)
\end{aligned}$$

$$B(x) = x \cos(x) - \sin(x)$$

$$\tilde{B}(x) = x \sin(x) + \cos(x)$$

$$C(u) = \left[\left(\frac{y^2}{2} - z^2 \right) u \cos(u) + \left(x^2 + \frac{y^2}{2}(u^2 - 1) \right) \sin(u) \right]$$

$$\tilde{C}(u) = \left[\left(\frac{y^2}{2} - z^2 \right) u \sin(u) - \left(x^2 + \frac{y^2}{2}(u^2 - 1) \right) \cos(u) \right]$$

$$D(u) = \left[(x^2 - 2y^2) u \cos(u) + (2y^2 + x^2(u^2 - 1)) \sin(u) \right]$$

$$\tilde{D}(u) = \left[(x^2 - 2y^2) u \sin(u) - (2y^2 + x^2(u^2 - 1)) \cos(u) \right]$$

One can easily verify that the corrections b^{ij} and h^{ij} induced by the presence of the conducting plate vanish for long enough distances of the particles to it, as they behave as inverse powers of this distance.

Appendix B: Reduced density matrix elements

Herein, we show the analytic expression of the components of the reduced density matrix elements, after having solved the master equation Eq.(7) by assuming an initial quantum state of the form $|\psi\rangle = \alpha|11\rangle + \beta|10\rangle + \gamma|01\rangle + \sigma|00\rangle$:

$$\begin{aligned}
\rho_{11}(t) &= \alpha^2 e^{-4\Gamma^{11}} \\
\rho_{41}(t) &= \sigma^* \alpha e^{-2\Gamma^{11}} e^{2i(\gamma^{11} + \omega_0 t)} \\
\begin{pmatrix} \rho_{21} \\ \rho_{31} \end{pmatrix} &= \left[\frac{(\beta + \delta)\alpha}{2} \begin{pmatrix} 1 \\ 1 \end{pmatrix} e^{-\Gamma^{12}} e^{-i\gamma^{12}} + \frac{(\beta - \delta)\alpha}{2} \begin{pmatrix} 1 \\ -1 \end{pmatrix} e^{\Gamma^{12}} e^{i\gamma^{12}} \right] e^{-3\Gamma^{11}} e^{i(\gamma^{11} + \omega_0 t)} \\
\begin{pmatrix} \rho_{42} \\ \rho_{43} \end{pmatrix} &= \left[\frac{(\sigma + \alpha G'(t))(\beta + \delta)}{2} \begin{pmatrix} 1 \\ 1 \end{pmatrix} e^{-\Gamma^{12}} e^{i\gamma^{12}} + \frac{(\sigma + \alpha F'(t))(\beta - \delta)}{2} \begin{pmatrix} 1 \\ -1 \end{pmatrix} e^{\Gamma^{12}} e^{-i\gamma^{12}} \right] e^{-\Gamma^{11}} e^{i(\gamma^{11} + 2\omega_0 t)} \\
\begin{pmatrix} \rho_{22} \\ \rho_{23} \\ \rho_{32} \\ \rho_{33} \end{pmatrix} &= \left[\left(\alpha^2 F(t) + \frac{(\beta - \delta)^2}{4} \right) \begin{pmatrix} 1 \\ -1 \\ -1 \\ 1 \end{pmatrix} e^{2\Gamma^{12}} + \left(\alpha^2 G(t) + \frac{(\beta + \delta)^2}{4} \right) \begin{pmatrix} 1 \\ 1 \\ 1 \\ 1 \end{pmatrix} e^{-2\Gamma^{12}} \right] e^{-2\Gamma^{11}} + \\
&\quad + \frac{-\beta^2 + \delta^2}{2} \begin{pmatrix} -\cos 2\gamma^{12} \\ -i \sin 2\gamma^{12} \\ i \sin 2\gamma^{12} \\ \cos 2\gamma^{12} \end{pmatrix} e^{-2\Gamma^{11}},
\end{aligned} \tag{B1}$$

The time dependent factors appearing in these expressions are obtained after tracing out the degrees of freedom of the environment

$$\begin{aligned}
\Gamma^{ij} &= \int_0^t dt' a_{ij}(t'), \\
\gamma^{ij} &= \int_0^t dt' c_{ij}(t'), \\
F'(t) &= \int_0^t dt' [a_{11}(t') - a_{12}(t')] e^{-2(\Gamma^{11} - i\gamma^{12})},
\end{aligned} \tag{B2}$$

$$\begin{aligned}
G'(t) &= \int_0^t dt' [a_{11}(t') + a_{12}(t')] e^{-2(\Gamma^{11} + i\gamma^{12})}, \\
F(t) &= \int_0^t dt' [a_{11}(t') - a_{12}(t')] e^{-2(\Gamma^{11} + \Gamma^{12})}, \\
G(t) &= \int_0^t dt' [a_{11}(t') + a_{12}(t')] e^{-2(\Gamma^{11} - \Gamma^{12})}.
\end{aligned} \tag{B3}$$

-
- [1] M. V. Berry, Proceedings of the Royal Society of London. Series A, Mathematical and Physical Sciences **392**, 45 (1984).
 - [2] S. Pancharatnam, Proceedings of the Indian Academy of Sciences - Section A **44**, 398 (1956).
 - [3] F. C. Lombardo and P. I. Villar, Phys. Rev. A **74**, 042311 (2006).
 - [4] F. C. Lombardo and P. I. Villar, International Journal of Quantum Information **06**, 707 (2008).
 - [5] P. I. Villar, Physics Letters A **373**, 206 (2009).
 - [6] P. I. Villar and F. C. Lombardo, Phys. Rev. A **83**, 052121 (2011).
 - [7] F. C. Lombardo and P. I. Villar, Phys. Rev. A **87**, 032338 (2013).
 - [8] F. C. Lombardo and P. I. Villar, Phys. Rev. A **89**, 012110 (2014).
 - [9] F. C. Lombardo and P. I. Villar, Phys. Rev. A **91**, 042111 (2015).
 - [10] F. M. Cucchietti, J.-F. Zhang, F. C. Lombardo, P. I. Villar, and R. Laflamme, Phys. Rev. Lett. **105**, 240406 (2010).
 - [11] P. J. Leek, J. M. Fink, A. Blais, R. Bianchetti, M. Göppl, J. M. Gambetta, D. I. Schuster, L. Frunzio, R. J. Schoelkopf, and A. Wallraff, Science **318**, 1889 (2007).
 - [12] E. Martín-Martínez, I. Fuentes, and R. B. Mann, Phys. Rev. Lett. **107**, 131301 (2011).
 - [13] H. Zhai, J. Zhang, and H. Yu, Annals of Physics **371**, 338 (2016).
 - [14] J. Hu and H. Yu, Phys. Rev. A **85**, 032105 (2012).
 - [15] F. C. Lombardo and P. I. Villar, EPL (Europhysics Letters) **118**, 50003 (2017).
 - [16] C. H. Bennett and S. J. Wiesner, Phys. Rev. Lett. **69**, 2881 (1992).
 - [17] C. H. Bennett, P. W. Shor, J. A. Smolin, and A. V. Thapliyal, Phys. Rev. Lett. **83**, 3081 (1999).
 - [18] T. Yu and J. H. Eberly, Science **323**, 598 (2009).
 - [19] L. Mazzola, S. Maniscalco, J. Piilo, and K.-A. Suominen, Journal of Physics B: Atomic, Molecular and Optical Physics **43**, 085505 (2010).
 - [20] Z. Ficek and R. Tanaś, Phys. Rev. A **74**, 024304 (2006).
 - [21] Y. Yang, J. Hu, and H. Yu, Phys. Rev. A **94**, 032337 (2016).
 - [22] S. Cheng, H. Yu, and J. Hu, Phys. Rev. D **98**, 025001 (2018).
 - [23] W. E. Lamb and R. C. Retherford, Phys. Rev. **72**, 241 (1947).
 - [24] H. B. Casimir, in *Proceedings of the KNAW*, Vol. 51 (1948) pp. 793–795.
 - [25] F. C. Lombardo and P. I. Villar, Phys. Rev. A **81**, 022115 (2010).
 - [26] L. E. Oxman, A. Z. Khoury, F. C. Lombardo, and P. I. Villar, Annals of Physics **390**, 159 (2018).
 - [27] P. W. Milonni, *The quantum vacuum: an introduction to quantum electrodynamics* (Academic press, 2013).
 - [28] H.-P. Breuer and F. Petruccione, *The theory of open quantum systems* (Oxford University Press on Demand, 2002).
 - [29] P. Haikka and S. Maniscalco, Phys. Rev. A **81**, 052103 (2010).
 - [30] F. D. Mazzitelli, J. P. Paz, and A. Villanueva, Phys. Rev. A **68**, 062106 (2003).
 - [31] W. K. Wootters, Phys. Rev. Lett. **80**, 2245 (1998).
 - [32] R. L. Franco, B. Bellomo, S. Maniscalco, and G. Compagno, International Journal of Modern Physics B **27**, 1345053 (2013).
 - [33] D. M. Tong, E. Sjöqvist, L. C. Kwek, and C. H. Oh, Phys. Rev. Lett. **93**, 080405 (2004).
 - [34] D. M. Tong, E. Sjöqvist, L. C. Kwek, and C. H. Oh, Phys. Rev. Lett. **95**, 249902 (2005).
 - [35] H. Yu and J. Hu, Phys. Rev. A **86**, 064103 (2012).